Measurements of Parity-Violating Asymmetries in Electron-Deuteron Scattering in the Nucleon Resonance Region

Measurements of Parity-Violating Asymmetries in Electron-Deuteron Scattering in the Nucleon Resonance Region

D. Wang,[1] K. Pan,[2] R. Subedi,[1,†] X. Deng,[1] Z. Ahmed,[3] K. Allada,[4] K. A. Aniol,[5] D. S. Armstrong,[6] J. Arrington,[7] V. Bellini,[8] R. Beminiwattha,[9] J. Benesch,[10] F. Benmokhtar,[11] A. Camsonne,[10] M. Canan,[12] G. D. Cates,[1] J.-P. Chen,[10] E. Chudakov,[10] E. Cisbani,[13] M. M. Dalton,[1] C. W. de Jager,[10,1] R. De Leo,[14] W. Deconinck,[6] A. Deur,[10] C. Dutta,[4] L. El Fassi,[15] D. Flay,[16] G. B. Franklin,[11] M. Friend,[11] S. Frullani,[13] F. Garibaldi,[13] A. Giusa,[8] A. Glamazdin,[17] S. Golge,[12] K. Grimm,[18] K. Hafidi,[7] O. Hansen,[10] D. W. Higinbotham,[10] R. Holmes,[3] T. Holmstrom,[19] R. J. Holt,[7] J. Huang,[2] C. E. Hyde,[12,20] C. M. Jen,[3] D. Jones,[1] H. Kang,[21] P. King,[9] S. Kowalski,[2] K. S. Kumar,[22] J. H. Lee,[6,9] J. J. LeRose,[10] N. Liyanage,[1] E. Long,[23] D. McNulty,[22,‡] D. J. Margaziotis,[5] F. Meddi,[24] D. G. Meekins,[10] L. Mercado,[22] Z.-E. Meziani,[16] R. Michaels,[10] M. Mihovilovic,[25] N. Muangma,[2] K. E. Myers,[26,§] S. Nanda,[10] A. Narayan,[27] V. Nelyubin,[1] Nuruzzaman,[27] Y. Oh,[21] D. Parno,[11] K. D. Paschke,[1] S. K. Phillips,[28] X. Qian,[29] Y. Qiang,[29] B. Quinn,[11] A. Rakhman,[3] P. E. Reimer,[7] K. Rider,[19] S. Riordan,[1] J. Roche,[9] J. Rubin,[7] G. Russo,[8] K. Saenboonruang,[1,∥] A. Saha,[10,*] B. Sawatzky,[10] A. Shahinyan,[30] R. Silwal,[1] S. Sirca,[25] P. A. Souder,[3] R. Suleiman,[10] V. Sulkosky,[2] C. M. Sutera,[8] W. A. Tobias,[1] G. M. Urciuoli,[24] B. Waidyawansa,[9] B. Wojtsekhowski,[10] L. Ye,[31] B. Zhao,[6] and X. Zheng[1,¶]

(Jefferson Lab Hall A Collaboration)

[1]*University of Virginia, Charlottesville, Virginia 22904, USA*
[2]*Massachusetts Institute of Technology, Cambridge, Massachusetts 02139, USA*
[3]*Syracuse University, Syracuse, New York 13244, USA*
[4]*University of Kentucky, Lexington, Kentucky 40506, USA*
[5]*California State University, Los Angeles, Los Angeles, California 90032, USA*
[6]*College of William and Mary, Williamsburg, Virginia 23187, USA*
[7]*Physics Division, Argonne National Laboratory, Argonne, Illinois 60439, USA*
[8]*Istituto Nazionale di Fisica Nucleare, Dipartimento di Fisica dell'Università di Catania, I-95123 Catania, Italy*
[9]*Ohio University, Athens, Ohio 45701, USA*
[10]*Thomas Jefferson National Accelerator Facility, Newport News, Virginia 23606, USA*
[11]*Carnegie Mellon University, Pittsburgh, Pennsylvania 15213, USA*
[12]*Old Dominion University, Norfolk, Virginia 23529, USA*
[13]*INFN, Sezione di Roma, gruppo Sanità and Istituto Superiore di Sanità, I-00161 Rome, Italy*
[14]*Università di Bari, I-70126 Bari, Italy*
[15]*Rutgers, The State University of New Jersey, Newark, New Jersey 07102, USA*
[16]*Temple University, Philadelphia, Pennsylvania 19122, USA*
[17]*Kharkov Institute of Physics and Technology, Kharkov 61108, Ukraine*
[18]*Louisiana Technical University, Ruston, Louisiana 71272, USA*
[19]*Longwood University, Farmville, Virginia 23909, USA*
[20]*Clermont Université, Université Blaise Pascal, CNRS/IN2P3, Laboratoire de Physique Corpusculaire, FR-63000 Clermont-Ferrand, France*
[21]*Seoul National University, Seoul 151-742, South Korea*
[22]*University of Massachusetts Amherst, Amherst, Massachusetts 01003, USA*
[23]*Kent State University, Kent, Ohio 44242, USA*
[24]*INFN, Sezione di Roma and Sapienza Università di Roma, I-00161 Rome, Italy*
[25]*Institut Jožef Stefan, 3000 SI-1001 Ljubljana, Slovenia*
[26]*George Washington University, Washington, D.C. 20052, USA*
[27]*Mississippi State University, Starkeville, Mississippi 39762, USA*
[28]*University of New Hampshire, Durham, New Hampshire 03824, USA*
[29]*Duke University, Durham, North Carolina 27708, USA*
[30]*Yerevan Physics Institute, Yerevan 0036, Armenia*
[31]*China Institute of Atomic Energy, Beijing, 102413, People's Republic of China*
(Received 29 April 2013; published 22 August 2013)

We report on parity-violating asymmetries in the nucleon resonance region measured using inclusive inelastic scattering of 5–6 GeV longitudinally polarized electrons off an unpolarized deuterium target. These results are the first parity-violating asymmetry data in the resonance region beyond the $\Delta(1232)$. They provide a verification of quark-hadron duality—the equivalence of the quark- and hadron-based pictures of the nucleon—at the (10–15)% level in this electroweak observable, which is dominated by contributions from the nucleon electroweak γZ interference structure functions. In addition, the results provide constraints on nucleon resonance models relevant for calculating background corrections to elastic parity-violating electron scattering measurements.

DOI: 10.1103/PhysRevLett.111.082501 PACS numbers: 12.15.Ji, 14.20.Gk, 25.30.Dh

While QCD is the well-established theory of the strong nuclear force, it remains a challenge to describe the transition from quark and gluon to hadron degrees of freedom. Measurements of the structure functions in electron scattering from nuclei, spanning from the low invariant mass regime ($W < 2$ GeV) of resonance production to the deep inelastic scattering (DIS) regime, aim to bridge this transition. Inclusive measurements from nucleons have demonstrated a remarkable feature called ‘‘quark-hadron duality,’’ first pointed out by Bloom and Gilman [1], in which the low-energy (few GeV) cross sections averaged over the energy intervals of the resonance structures resemble those at asymptotically high energies. Over the past decade, duality has been verified in the unpolarized structure functions F_2 and F_L at four-momentum-transfer-squared Q^2 values below 1 $(\mathrm{GeV}/c)^2$ [2–6], the proton spin asymmetry A_1^p down to $Q^2 = 1.6$ $(\mathrm{GeV}/c)^2$ [7], the spin structure function g_1 down to $Q^2 = 1.7$–$1.8\,(\mathrm{GeV}/c)^2$ [8,9], the helicity-dependent structure functions $H_{1/2,3/2}$ [10], and for charged pion electroproduction in semi-inclusive scattering [11]. It was speculated that duality is a universal feature of the quark-hadron transition that should be exhibited not only in electromagnetic interactions but also in charged lepton scattering via the weak interaction [12], and perhaps other processes as well. Soon after duality was first observed, attempts were made to understand it from the first principles of QCD [13], and it is even more desired now, given such solid experimental verification. For a recent review of both the experimental and theoretical status of duality, see Ref. [14]. Establishing duality, either experimentally or theoretically, also has practical advantages for the study of nucleon structure. For example, the valence quark structure which is typically difficult to explore due to the high Q^2 required in DIS may be studied alternatively by averaging resonance data at lower Q^2 values [5,6,10,15,16].

To study quark-hadron duality in weak interactions, it is natural to start with parity-violating electron scattering (PVES) asymmetries $A_{\mathrm{PV}} = (\sigma_R - \sigma_L)/(\sigma_R + \sigma_L)$, where $\sigma_{R(L)}$ is the cross section for electrons polarized parallel (antiparallel) to their momentum. The PVES asymmetry on a nucleon or nuclear target is dominated by the electroweak γZ interference structure functions [17]:

$$A_{\mathrm{PV}} = \left(\frac{G_F Q^2}{4\sqrt{2}\pi\alpha}\right)\left(2g_A^e Y_1 \frac{F_1^{\gamma Z}}{F_1^{\gamma}} + g_V^e Y_3 \frac{F_3^{\gamma Z}}{F_1^{\gamma}}\right). \qquad (1)$$

Here, G_F is the Fermi weak coupling constant, α is the fine structure constant, Y_1 and Y_3 are kinematic factors, $g_{V,A}^e$ are the $e - Z^0$ vector and axial couplings, and $F_{1,3}^{\gamma,\gamma Z}$ are the electromagnetic and the γZ interference structure functions. Note that the γZ functions depend also on $g_{V,A}^q$, the quark-Z^0 vector, and axial couplings. In the standard model, the electron (quark) vector and axial couplings are related to the electron's (quark's) quantum numbers and the weak mixing angle $\sin^2\theta_W$. In practice, the structure functions $F_{1,3}^{\gamma,\gamma Z}$ are calculated using either parton distribution functions (for deep inelastic scattering) or nucleon and nuclear models (for elastic scattering or nucleon resonances), which provide predictions for asymmetries that can be compared with the measured values, to either allow extraction of electroweak parameters such as $\sin^2\theta_W$ or to test models used in structure function calculations. The first PVES experiment [18] provided the first measurement of $\sin^2\theta_W$ and established the $SU(2) \times U(1)$ gauge model of Weinberg, Glashow, and Salam [19] as the correct theory for electroweak interactions. In the past decade, with the increasing precision accessible to modern experiments [20], PVES has become a powerful tool to measure not only $\sin^2\theta_W$ but also $g_{A,V}^{e,q}$ through DIS measurements [21], the nucleon strange form factors via elastic scattering [22–26] (for a review, see Ref. [27]), the weak charge and neutron densities of nuclei [28,29], and possibly isospin symmetry violation in the parton distribution functions (PDFs) [30,31]. However, measurements of the PVES asymmetry in the nucleon resonance region are scarce. The only existing data are from the $G0$ experiment, in which the asymmetry was measured from a proton target near the $\Delta(1232)$ region with statistical and systematic uncertainties of approximately 15% each [32].

Measurements of PVES asymmetries in the resonance region will also help to test our understanding of the structure of nucleon resonances. In the resonance region, the PV structure functions can be described in terms of longitudinal, transverse, and axial PV response functions to specific resonance states, together with a nonresonant background. These electroweak structure functions can be decomposed in terms of their isospin content, providing new and unique sensitivity to combinations of quark currents weighted by their electroweak couplings to the incident electrons [33]. The asymmetry for the first nucleon resonance, the $N \to \Delta(1232)$ transition, was first calculated by Cahn and Gilman [17]. Subsequently, more precise calculations in the resonance region have been performed [33]. Based on these calculations, the $\Delta(1232)$ asymmetry from the proton reported by $G0$ was used to extract the axial form factor $G_{N\Delta}^A$ [32].

In this Letter, we present parity-violating asymmetries for scattering longitudinally polarized electrons from an unpolarized deuterium target at four combinations of Q^2 and invariant mass W spanning the whole nucleon resonance region, obtained during a recent experiment [21] at the Thomas Jefferson National Accelerator Facility (JLab). These results provide a test of local quark-hadron duality in the nucleon electroweak γZ interference structure functions and are compared to the theoretical models of Matsui, Sato, and Lee [34], Gorchtein, Horowitz, and Ramsey-Musolf [35], and the Adelaide-JLab-Manitoba Collaboration [36]. These results also provide constraints for nucleon resonance models relevant for calculating background corrections to elastic PVES [35–40].

The experiment was performed in experimental Hall A of JLab. A 100–105 μA polarized electron beam was incident on a liquid deuterium target, and scattered events were detected by the Hall A high resolution spectrometer (HRS) pair [41] in inclusive mode. The main goal of the experiment was to provide precision PV asymmetries in the DIS region as a test of the standard model [42] and to extract the quark weak axial charges C_{2q} [21]; those measurements will be reported in future publications. The results reported here come from additional data collected in the nucleon resonance region during this experiment: kinematics I–IV were centered at $W = 1.263$, 1.591, 1.857, and 1.981 GeV, respectively. The Q^2 values were just below 1 $(\mathrm{GeV}/c)^2$ except for kinematics IV, which was at $Q^2 = 1.472$ $(\mathrm{GeV}/c)^2$. The beam energies were 4.867 GeV for kinematics I–III and 6.067 GeV for IV.

The polarized electron beam was produced by illuminating a strained GaAs photocathode with circularly polarized laser light. The helicity of the electron beam was selected from a pseudorandom [23] sequence every 66 ms and reversed in the middle of this time window, forming helicity pairs. The data acquisition was gated by this helicity sequence. To reduce possible systematic errors, a half-wave plate was inserted intermittently into the path of the polarized laser, which resulted in a reversal of the actual beam helicity while keeping the helicity sequence unchanged. The expected sign flips in the measured asymmetries between the two beam half-wave-plate configurations were observed. The laser optics of the polarized source were carefully configured to minimize changes to the electron-beam parameters under polarization reversal [43]. A feedback system [44] was used to maintain the helicity-correlated intensity asymmetry of the beam below 0.1 parts per million (ppm) averaged over the whole experiment. The target was a 20-cm-long liquid deuterium cell, with up- and downstream windows made of 0.10- and 0.13-mm-thick aluminum, respectively.

In order to count the up-to-600-kHz electron rate and reject the pion photo- and electroproduction backgrounds, a data acquisition (DAQ) and electronic system was specially designed for this experiment and formed both electron and pion triggers. The design of the DAQ, along with its particle identification performance and the dead time corrections to the measured asymmetries, was reported elsewhere [45]. The overall charged pion π^- contamination was found to contribute less than 4×10^{-4} of the detected electron rate. Using the measured asymmetries from the pion triggers, the relative uncertainty on the measured electron asymmetries $\Delta A/A$ due to the π^- background was evaluated to be less than 5×10^{-4}. Relative corrections on the asymmetry due to DAQ dead time were (0.7–2.5)% with uncertainties $\Delta A/A < 0.5\%$. The standard HRS DAQ [41] was used at low beam currents to precisely determine the kinematics of the experiment. This was realized through dedicated measurements on a carbon multifoil target which provided data to determine the transport function of the HRSs.

The number of scattered particles in each helicity window was normalized to the integrated charge from the beam current monitors, from which the raw asymmetries A_{raw} were formed. The raw asymmetries were then corrected for helicity-dependent fluctuations in the beam parameters, following $A^{\mathrm{bc}}_{\mathrm{raw}} = A_{\mathrm{raw}} - \sum c_i \Delta x_i$, where Δx_i are the measured helicity window differences in the beam position, angle, and energy. The values of the correction coefficients c_i could be extracted either from natural movement of the beam or from calibration data collected during the experiment, in which the beam was modulated several times per hour using steering coils and an accelerating cavity. The largest of the corrections was approximately 0.4 ppm, and the difference between the two methods was used to estimate the systematic uncertainty in the beam corrections.

The beam-corrected asymmetries $A^{\mathrm{bc}}_{\mathrm{raw}}$ were then corrected for the beam polarization. The longitudinal polarization of the electron beam was measured intermittently during the experiment by a Møller polarimeter [41], with a result of $P_b = (90.40 \pm 1.54)\%$ for kinematics I–III and $(89.88 \pm 1.80)\%$ for IV. In both cases, the uncertainty was dominated by the knowledge of the Møller target polarization. The Compton polarimeter [46] measured $(89.45 \pm 1.71)\%$ for kinematics IV where the uncertainty came primarily from the limit in understanding the analyzing power but was not available for kinematics I–III. The Møller and Compton measurements for kinematics IV were combined to give $(89.65 \pm 1.24)\%$. The passage of the beam through material before scattering causes a small depolarization effect that was corrected. This was calculated based on Ref. [47], and the beam depolarization was found to be less than 6.1×10^{-4} for all resonance kinematics.

Next, the asymmetries were corrected for various backgrounds. The pair-production background, which results from π^0 decays, was measured at the DIS kinematics of this experiment by reversing the polarity of the HRS magnets and was found to contribute less than 5×10^{-3} of the detected rate. Since pion production is smaller in resonance kinematics than in DIS, and based on the fact that pions were produced at lower Q^2 than electrons of the same momentum and hence typically have smaller PV asymmetries, the relative uncertainty on the measured asymmetries due to this background was estimated to be no more than 5×10^{-3}. Background from the aluminum target windows was estimated using Eq. (1), with structure functions $F_{1,3}^{\gamma Z}$ for aluminum constructed from the MSTW DIS PDF [48] extrapolated to the measured $\langle Q^2 \rangle$ and $\langle W \rangle$ values, and the latest world fit on the ratio of longitudinal to transverse virtual photon electromagnetic absorption cross sections $R \equiv \sigma_L/\sigma_T$ [49]. Assuming that the actual asymmetries differ by no more than 20% from calculated values due to resonance structure and nuclear effects, the relative correction to the asymmetry is at the (1–3) $\times 10^{-4}$ level with an uncertainty of $\Delta A/A = 0.4\%$ for all kinematics. Target impurity adds about 0.06% of relative uncertainty to the measured asymmetry due to the presence of a small amount of hydrogen deuteride. Background from events rescattering off the inner walls of the HRS was estimated using the probability of such rescattering and adds no more than 1% relative uncertainty to the measured asymmetry.

Corrections from the beam polarization in the direction perpendicular to the scattering plane can be described as $\delta A = A_n[-S_H \sin\theta_{\rm tr} + S_V \cos\theta_{\rm tr}]$, where A_n is the beam-normal asymmetry, $S_{V,H,L}$ are, respectively, the electron polarization components in the vertical, horizontal, and longitudinal directions, and $\theta_{\rm tr}$ is the vertical angle of the scattered electrons. During the experiment, the beam spin components were controlled to $|S_H/S_L| \leq 27.4\%$ and $|S_V/S_L| \leq 2.5\%$, and the value of $\theta_{\rm tr}$ was found to be less than 0.01 rad. Therefore, the beam vertical spin dominates this background: $\delta A \approx A_n S_V \cos\theta_{\rm tr} \leq (2.5\%) P_b A_n$, where $P_b = S_L$ is the beam longitudinal polarization described earlier. The values of A_n were measured at DIS kinematics and were found to be consistent with previous measurements from electron elastic scattering from the proton and heavier nuclei [50]. Based on this, it was estimated that for resonance kinematics, A_n varies between -38 and -80 ppm depending on the value of Q^2, and its amplitude is always smaller than that of the corresponding measured electron asymmetry. Therefore, the uncertainty due to A_n was estimated to be no more than 2.5% of the measured asymmetries.

Radiative corrections were performed for both internal and external bremsstrahlung as well as ionization loss. External radiative corrections were performed based on the procedure first described by Mo and Tsai [51]. As inputs to the radiative corrections, PV asymmetries of elastic scattering from the deuteron were estimated using Ref. [52] and those from quasielastic scattering were based on Ref. [24]. The simulation used to calculate the radiative correction also takes into account the effect of HRS acceptance and particle identification efficiency variation across the acceptance.

Box-diagram corrections refer to effects that arise when the electron simultaneously exchanges two bosons ($\gamma\gamma$, γZ, or ZZ box) with the target, and they are dominated by the $\gamma\gamma$ and the γZ box diagrams. For PVES asymmetries, the box-diagram effects include those from the interference between Z exchange and the $\gamma\gamma$ box, the interference between γ exchange and the γZ box, and the effect of the $\gamma\gamma$ box on the electromagnetic cross sections. It is expected that there is at least partial cancellation among these three terms. The box-diagram corrections were estimated to be at the (0–1)% level [53], and a $(0.5 \pm 0.5)\%$ relative correction was applied to the asymmetries.

Results on the physics asymmetry $A_{\rm PV}^{\rm phys}$ were formed from the beam-corrected asymmetry $A_{\rm raw}^{\rm bc}$ by correcting for the beam polarization P_b and backgrounds with asymmetry A_i and fraction f_i, described above, using the equation

$$A_{\rm PV}^{\rm phys} = \frac{(\frac{A_{\rm raw}^{\rm bc}}{P_b} - \sum_i A_i f_i)}{1 - \sum_i f_i}. \quad (2)$$

When all f_i are small with A_i comparable to or smaller than $A_{\rm raw}^{\rm bc}$, one can define $\bar{f}_i = f_i(1 - (A_i/A_{\rm raw}^{\rm bc})P_b)$ and approximate

$$A_{\rm PV}^{\rm phys} \approx \frac{A_{\rm raw}^{\rm bc}}{P_b} \Pi_i (1 + \bar{f}_i); \quad (3)$$

i.e., all corrections can be treated as multiplicative.

Table I shows all kinematics, the beam-corrected asymmetries $A_{\rm raw}^{\rm bc}$, and the final asymmetry results $A_{\rm PV}^{\rm phys}$ compared to calculations from Matsui, Sato, and Lee [34] [for $\Delta(1232)$ only], Gorchtein, Horowitz, and Ramsey-Musolf [35], and the Adelaide-JLab-Manitoba model [36]. In addition, the structure functions $F_{1,3}^{\gamma(Z)}$ in Eq. (1) can be estimated using PDF fits obtained from DIS data, extrapolated to the resonance region, along with the quark-Z^0 vector and axial couplings $g_{V,A}^q$ based on standard model values [42]. This approach provides DIS estimations $A_{\rm calc}^{\rm DIS}$ that can be compared to the measured asymmetries to test quark-hadron duality. For these DIS estimations, electroweak radiative corrections were applied to $g_{V,A}^q$ directly, and three PDF fits—MSTW [48], CTEQ-Jefferson Lab (CJ) [54], and CT10 [55]—extrapolated to the measured $\langle Q^2 \rangle$ and $\langle W \rangle$ values were used along with world data on R [49]. The uncertainty from each PDF fit was below a fraction of a ppm, and the differences among all three fits were below 1.5 ppm for all kinematics. From Table I, one can see that the final asymmetry results agree very well with the DIS calculations, indicating that for the Q^2 range covered by these measurements, duality holds throughout the whole resonance region at the (10–15)% level.

In addition to the results in Table I, asymmetry results with smaller bins in W are also available due to the detector segmentation and trigger electronics adopted in this experiment [45]: for each kinematics, six (eight) "group" triggers were formed first from different segments of the

TABLE I. Asymmetry results on parity-violating $\vec{e} - {}^2$H scattering in the nucleon resonance region. The kinematics shown include the beam energy E_b, with which HRS was used (left or right), the central angle and momentum settings of the HRS θ_0 and p_0, and the actual kinematics averaged from the data $\langle Q^2 \rangle$ and $\langle W \rangle$. The beam-corrected asymmetries $A_{\rm raw}^{\rm bc}$ are shown along with their statistical precision and systematic uncertainties due to beam-related corrections. Final results on the physics asymmetries $A_{\rm PV}^{\rm phys}$ are compared with calculations from three resonance models [34–36] as well as DIS estimations using CJ [54] PDF fits $A_{\rm calc}^{\rm DIS,CJ}$.

Kinematics	I	II	III	IV
E_b (GeV)	4.867	4.867	4.867	6.067
HRS	Left	Left	Right	Left
θ_0	12.9°	12.9°	12.9°	15.0°
p_0 (GeV/c)	4.00	3.66	3.10	3.66
$\langle Q^2 \rangle$ [(GeV/c)^2]	0.950	0.831	0.757	1.472
$\langle W \rangle$ (GeV)	1.263	1.591	1.857	1.981
Measured asymmetries with beam-related corrections (ppm)				
$A_{\rm raw}^{\rm bc}$	−55.11	−63.75	−54.38	−104.04
$\pm\Delta A_{\rm raw}^{\rm bc}$ (stat)	±6.77	±5.91	±4.47	±15.26
$\pm\Delta A_{\rm raw}^{\rm bc}$ (syst)	±0.10	±0.15	±0.24	±0.26
Physics asymmetry results (ppm)				
$A_{\rm PV}^{\rm phys}$	−68.97	−74.12	−61.80	−119.56
$\pm\Delta A_{\rm PV}^{\rm phys}$(stat)	±8.47	±6.87	±5.08	±17.54
$\pm\Delta A_{\rm PV}^{\rm phys}$(syst)	±3.30	±2.84	±2.11	±5.62
$\pm\Delta A_{\rm PV}^{\rm phys}$(total)	±9.09	±7.43	±5.50	±18.42
Calculations (ppm)				
$A_{\rm calc}$ [34]	−89.10	...	...	...
$A_{\rm calc}$	−88.94	−70.29	−65.09	−124.74
$\pm\Delta A_{\rm calc}$ [35]	$^{+9.98}_{-8.76}$	$^{+14.81}_{-11.09}$	$^{+11.85}_{-10.95}$	$^{+20.12}_{-19.49}$
$A_{\rm calc}$	−88.22	−69.63	−65.23	−124.75
$\pm\Delta A_{\rm calc}$ [36]	$^{+8.10}_{-8.31}$	$^{+7.05}_{-7.19}$	$^{+5.19}_{-5.34}$	$^{+9.11}_{-9.49}$
$A_{\rm calc}^{\rm DIS,CJ}$	−75.63	−66.72	−61.59	−119.13

detectors for the left (right) HRS, and a logical "or" of all group triggers was formed to give a global trigger. While asymmetry results from the global trigger, shown in Table I, provided higher statistical precision, asymmetries extracted from group triggers allowed study of the detailed W dependence of the asymmetry within each kinematic setting, with little variation in Q^2. Figure 1 shows the W dependence of asymmetry results $A_{\rm PV}^{\rm phys}$, scaled by $1/Q^2$, extracted from group triggers. The data between adjacent bins within each kinematics typically have a (20–30)% overlap in event samples and are thus correlated, while the lowest and the highest bins of each kinematics have larger overlaps with their adjacent bins.

One can see from Fig. 1 that the measured asymmetries at all kinematics are consistent with the three resonance models and again agree very well with the DIS estimation. No significant resonance structure is observed in the W dependence of the asymmetries.

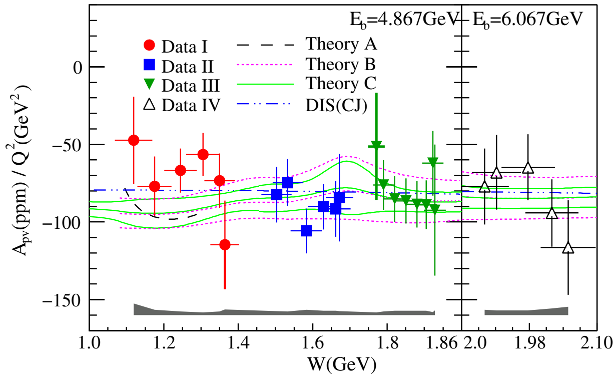

FIG. 1 (color online). W dependence of the parity-violating asymmetries in $\vec{e} - {}^2$H scattering extracted from this experiment. The physics asymmetry results $A_{\rm PV}^{\rm phys}$ for the four kinematics I, II, III, and IV (solid circles, solid squares, solid triangles, and open triangles, respectively), in ppm, are scaled by $1/Q^2$ and compared with calculations from Ref. [34] (theory A, dashed lines), Ref. [35] (theory B, dotted lines), Ref. [36] (theory C, solid lines), and the DIS estimation (dash-double-dotted lines) using Eq. (1) with the extrapolated CJ PDF [54]. The vertical error bars for the data are statistical uncertainties, while the horizontal error bars indicate the root-mean-square values of the W coverage of each bin. The experimental systematic uncertainties are shown as the shaded bands at the bottom. For each of the four kinematics, calculations were performed at the fixed E_b and Q^2 values of Table I and with a variation in W to match the coverage of the data. Theories B and C each have three curves showing the central values and the upper and lower bounds of the calculation. Uncertainties of the DIS calculation were below 1 ppm and are not visible.

In summary, we report here results on the parity-violating asymmetries in the nucleon resonance region, including the first PV asymmetry data beyond the $\Delta(1232)$ resonance. These results provide important constraints to nucleon resonance models relevant for calculating background corrections to elastic parity-violating electron scattering measurements. The agreement with DIS-based calculations indicates that quark-hadron duality holds for PVES asymmetries on the deuteron at the (10–15)% level throughout the resonance region, for Q^2 values just below 1 (GeV/c)^2. These results are comparable to the unpolarized electromagnetic structure function data which verified duality at the (5–10)% level for the proton and (15–20)% for the neutron at similar Q^2 values, although the unpolarized measurements provided better resolution in W and covered a broader kinematic range [5,6,10]. We have therefore provided the first experimental support for the hypothesis that quark-hadron duality is a universal property of nucleons in both their weak and their electromagnetic interactions.

The authors would like to thank the personnel of Jefferson Lab for their efforts which resulted in the successful completion of the experiment, and T.-S. H. Lee, T. Sato, M. Gorshteyn, N. Hall, W. Melnitchouk, and their collaborators for carrying out the nucleon resonance calculations. X. Zheng would like to thank the Medium Energy Physics Group at the Argonne National Lab for supporting her during the initial work of this experiment. This work was supported in part by the Jeffress Memorial Trust under Grant No. J-836, the U.S. National Science Foundation under Grant No. 0653347, and the U.S. Department of Energy under Awards No. DE-SC0003885 and No. DE-AC02-06CH11357. *Notice:* Authored by Jefferson Science Associates, LLC under U.S. DOE Contract No. DE-AC05-06OR23177. The U.S. Government retains a nonexclusive, paid-up, irrevocable, worldwide license to publish or reproduce this manuscript for U.S. Government purposes.

*Deceased.

†Present address: Richland College, Dallas County Community College District, Dallas, TX 75243, USA.

‡Present address: Idaho State University, Pocatello, ID 83201, USA.

§Present address: Rutgers, The State University of New Jersey, Newark, NJ 07102, USA.

‖Present address: Kasetsart University, Bangkok 10900, Thailand.

¶To whom correspondence should be addressed. xiaochao@jlab.org

[1] E. D. Bloom and F. J. Gilman, Phys. Rev. Lett. **25**, 1140 (1970).

[2] I. Niculescu *et al.*, Phys. Rev. Lett. **85**, 1186 (2000).

[3] Y. Liang *et al.*, arXiv:nucl-ex/0410027.

[4] A. Psaker, W. Melnitchouk, M. E. Christy, and C. Keppel, Phys. Rev. C **78**, 025206 (2008).

[5] S. P. Malace, Y. Kahn, W. Melnitchouk, and C. E. Keppel, Phys. Rev. Lett. **104**, 102001 (2010).

[6] S. P. Malace *et al.*, Phys. Rev. C **80**, 035207 (2009).

[7] A. Airapetian *et al.* (HERMES Collaboration), Phys. Rev. Lett. **90**, 092002 (2003).

[8] P. E. Bosted *et al.*, Phys. Rev. C **75**, 035203 (2007).

[9] P. Solvignon *et al.*, Phys. Rev. Lett. **101**, 182502 (2008).

[10] S. P. Malace, W. Melnitchouk, and A. Psaker, Phys. Rev. C **83**, 035203 (2011).

[11] T. Navasardyan *et al.*, Phys. Rev. Lett. **98**, 022001 (2007).

[12] C. E. Carlson and N. C. Mukhopadhyay, Phys. Rev. D **47**, R1737 (1993).

[13] O. Nachtmann, Nucl. Phys. **B63**, 237 (1973); H. Georgi and H. D. Politzer, Phys. Rev. D **14**, 1829 (1976); A. De Rujula, H. Georgi, and H. D. Politzer, Phys. Lett. B **64**, 428 (1976).

[14] W. Melnitchouk, R. Ent, and C. Keppel, Phys. Rep. **406**, 127 (2005).

[15] J. Arrington, R. Ent, C. E. Keppel, J. Mammei, and I. Niculescu, Phys. Rev. C **73**, 035205 (2006).

[16] T. Averett, G. Cates, N. Liyanage, G. Rosner, B. Wojtsekhowski, X. Zheng *et al.*, Jefferson Lab Experiment No. 12-06-122, 2006.

[17] R. N. Cahn and F. J. Gilman, Phys. Rev. D **17**, 1313 (1978).

[18] C. Y. Prescott *et al.*, Phys. Lett. B **77**, 347 (1978); C. Y. Prescott *et al.*, Phys. Lett. B **84**, 524 (1979).

[19] S. L. Glashow, Nucl. Phys. **22**, 579 (1961); S. Weinberg, Phys. Rev. Lett. **19**, 1264 (1967); A. Salam, *Elementary Particle Theory*, edited by N. Svartholm (Almquist Forlag, Stockholm, 1968).

[20] D. S. Armstrong and R. D. McKeown, Annu. Rev. Nucl. Part. Sci. **62**, 337 (2012).

[21] X. Zheng, P. Reimer, R. Michaels *et al.*, Jefferson Lab Experiment No. 08-011, http://hallaweb.jlab.org/experiment/E08-011.

[22] R. D. Mckeown, Phys. Lett. B **219**, 140 (1989); D. T. Spayde *et al.*, Phys. Lett. B **583**, 79 (2004); T. M. Ito *et al.*, Phys. Rev. Lett. **92**, 102003 (2004).

[23] K. A. Aniol *et al.*, Phys. Lett. B **509**, 211 (2001); K. A. Aniol *et al.*, Phys. Rev. Lett. **96**, 022003 (2006); K. A. Aniol *et al.*, Phys. Lett. B **635**, 275 (2006); A. Acha *et al.*, Phys. Rev. Lett. **98**, 032301 (2007); Z. Ahmed *et al.*, Phys. Rev. Lett. **108**, 102001 (2012).

[24] K. A. Aniol *et al.*, Phys. Rev. C **69**, 065501 (2004).

[25] D. H. Beck, Phys. Rev. D **39**, 3248 (1989); D. S. Armstrong *et al.*, Phys. Rev. Lett. **95**, 092001 (2005); D. Androic *et al.*, Phys. Rev. Lett. **104**, 012001 (2010).

[26] F. E. Maas *et al.*, Phys. Rev. Lett. **93**, 022002 (2004); F. E. Maas *et al.*, Phys. Rev. Lett. **94**, 152001 (2005); S. Baunack *et al.*, Phys. Rev. Lett. **102**, 151803 (2009).

[27] K. Paschke, A. Thomas, R. Michaels, and D. Armstrong, J. Phys. Conf. Ser. **299**, 012003 (2011).

[28] S. Abrahamyan *et al.*, Phys. Rev. Lett. **108**, 112502 (2012).

[29] C. J. Horowitz *et al.*, Phys. Rev. C **85**, 032501 (2012).

[30] J. T. Londergan, J. C. Peng, and A. W. Thomas, Rev. Mod. Phys. **82**, 2009 (2010).

[31] I. C. Cloet, W. Bentz, and A. W. Thomas, Phys. Rev. Lett. **109**, 182301 (2012).

[32] D. Androic *et al.*, arXiv:1212.1637.

[33] M. J. Musolf, T. W. Donnelly, J. Dubach, S. J. Pollock, S. Kowalski, and E. J. Beise, Phys. Rep. **239**, 1 (1994); J. E. Amaro, M. B. Barbaro, J. A. Caballero, T. W. Donnelly, and A. Molinari, Phys. Rep. **368**, 317 (2002); M. B. Barbaro, J. A. Caballero, T. W. Donnelly, and C. Maieron, Phys. Rev. C **69**, 035502 (2004); A. De Pace, M. Nardi, W. M. Alberico, T. W. Donnelly, and A. Molinari, Nucl. Phys. **A741**, 249 (2004); S. L. Adler, Ann. Phys. (N.Y.) **50**, 189 (1968); D. R. T. Jones and S. T. Petcov, Phys. Lett. B **91**, 137 (1980); L. M. Nath, K. Schilcher, and M. Kretzschmar, Phys. Rev. D **25**, 2300 (1982).

[34] K. Matsui, T. Sato, and T.-S. H. Lee, Phys. Rev. C **72**, 025204 (2005).

[35] M. Gorchtein, C. J. Horowitz, and M. J. Ramsey-Musolf, Phys. Rev. C **84**, 015502 (2011); M. Gorchtein (private communication).

[36] N. L. Hall, P. G. Blunden, W. Melnitchouk, A. W. Thomas, and R. D. Young, Phys. Rev. D **88**, 013011 (2013).

[37] M. Gorchtein and C. J. Horowitz, Phys. Rev. Lett. **102**, 091806 (2009).

[38] A. Sibirtsev, P. G. Blunden, W. Melnitchouk, and A. W. Thomas, Phys. Rev. D **82**, 013011 (2010).

[39] P. G. Blunden, W. Melnitchouk, and A. W. Thomas, Phys. Rev. Lett. **107**, 081801 (2011); Phys. Rev. Lett. **109**, 262301 (2012).

[40] B. C. Rislow and C. E. Carlson, Phys. Rev. D **83**, 113007 (2011).
[41] J. Alcorn *et al.*, Nucl. Instrum. Methods Phys. Res., Sect. A **522**, 294 (2004).
[42] J. Beringer *et al.* (Particle Data Group Collaboration), Phys. Rev. D **86**, 010001 (2012).
[43] C. K. Sinclair, P. A. Adderley, B. M. Dunham, J. C. Hansknecht, P. Hartmann, M. Poelker, J. S. Price, P. M. Rutt, W. J. Schneider, and M. Steigerwald, Phys. Rev. ST Accel. Beams **10**, 023501 (2007); P. A. Adderley, J. Clark, J. Grames, J. Hansknecht, K. Surles-Law, D. Machie, M. Poelker, M. L. Stutzman, and R. Suleiman, Phys. Rev. ST Accel. Beams **13**, 010101 (2010).
[44] K. D. Paschke, Eur. Phys. J. A **32**, 549 (2007).
[45] R. Subedi, D. Wang, K. Pan, X. Deng, R. Michaels, P. E. Reimer, A. Shahinyan, B. Wojtsekhowski, and X. Zheng, Nucl. Instrum. Methods Phys. Res., Sect. A **724**, 90 (2013).
[46] M. Friend *et al.*, Nucl. Instrum. Methods Phys. Res., Sect. A **676**, 96 (2012); S. Escoffier *et al.*, Nucl. Instrum. Methods Phys. Res., Sect. A **551**, 563 (2005).
[47] H. Olsen and L. C. Maximon, Phys. Rev. **114**, 887 (1959).
[48] A. D. Martin, W. J. Stirling, R. S. Thorne, and G. Watt, Eur. Phys. J. C **63**, 189 (2009).
[49] P. E. Bosted and M. E. Christy, Phys. Rev. C **77**, 065206 (2008).
[50] S. Abrahamyan *et al.*, Phys. Rev. Lett. **109**, 192501 (2012).
[51] L. W. Mo and Y.-S. Tsai, Rev. Mod. Phys. **41**, 205 (1969).
[52] E. J. Beise, M. L. Pitt, and D. T. Spayde, Prog. Part. Nucl. Phys. **54**, 289 (2005); D. Abbott *et al.*, Eur. Phys. J. A **7**, 421 (2000); S. J. Pollock, Phys. Rev. D **42**, 3010 (1990); Phys. Rev. D **43**, 2447 (1991).
[53] P. Blunden (private communication).
[54] J. F. Owens, A. Accardi, and W. Melnitchouk, Phys. Rev. D **87**, 094012 (2013).
[55] H.-L. Lai, M. Guzzi, J. Huston, Z. Li, P. M. Nadolsky, J. Pumplin, and C.-P. Yuan, Phys. Rev. D **82**, 074024 (2010).